

Design Considerations for Series-Connected Distributed FACTS Converters

Harjeet Johal, *Student Member, IEEE*, and Deepak Divan, *Fellow, IEEE*

Abstract—The power grid is aging, and getting increasingly congested. Conventional solutions, such as flexible ac transmission systems (FACTS) can be used to control power flow on the grid. However, widespread adoption of this technology has been hampered by high costs and reliability concerns. The concept of distributed FACTS devices, as an alternative approach to realizing cost-effective power flow control, has been recently proposed. This paper discusses the design considerations for implementing distributed power control solutions on the power grid, with specific examples for series var compensation, and the significant impact it can have on grid utilization and system reliability. The ability to use mature power conversion techniques demonstrates the potential for low-cost implementation.

Index Terms—Active power flow control, distributed flexible ac transmission systems (D-FACTS), FACTS, series var compensation.

I. INTRODUCTION

THE POWER grid in the U.S. and in most parts of the world is aging and under increasing stress. The modern industrial infrastructure demands increasing amounts of affordable and reliable electricity. Yet, in a semiregulated utility environment and in the face of increasing public sentiment against locating power lines in their communities, the ability to use the existing asset base more effectively has become a critical issue [1].

The utilities have done a good job in ensuring the availability of reliable electricity. An important component of higher reliability is a gradual move from radial power distribution to a system that is increasingly networked. This allows faulted sections of the grid to be rapidly isolated, without sustained interruption of power supply to the vast majority of customers. The utility cannot effectively control how power flows on such a network. Furthermore, the first line that hits the thermal limit constrains the total power transfer capacity of the entire system, even when other lines in the system are only operating at a fraction of their capacity. Finally, the network topology changes continually, as

Paper IPCSD-07-038, presented at the 2005 Industry Applications Society Annual Meeting, Hong Kong, October 2–6, and approved for publication in the IEEE TRANSACTIONS ON INDUSTRY APPLICATIONS by the Industrial Power Converter Committee of the IEEE Industry Applications Society. Manuscript submitted for review June 4, 2006 and released for publication May 14, 2007. This work was supported in part by the Intelligent Power Infrastructure Consortium (IPIC) at the Georgia Institute of Technology.

The authors are with the School of Electrical and Computer Engineering, Georgia Institute of Technology, Atlanta, GA 30332-0250 USA (e-mail: gtg687n@mail.gatech.edu; harjeet.johal@gatech.edu; deepak.divan@ece.gatech.edu).

Color versions of one or more of the figures in this paper are available online at <http://ieeexplore.ieee.org>.

Digital Object Identifier 10.1109/TIA.2007.908174

lines, loads and generation are added and dropped. Maintaining system integrity under current conditions, as well as under (N-1) and (N-2) contingency conditions, creates a compelling need for controlling power flow on the network.

The “conventional” and technically proven approach for controlling power flow on the grid has been through the use of flexible ac transmission systems (FACTS) devices [2]. Shunt var compensators such as STATCONs represent the more cost-effective technology. Shunt vars provide grid voltage support, while series vars are required to control active power flow. Active power flow requires “series var” solutions, that can alter the impedance of the power lines or change the angle of the voltage applied across the line [3], [4]. Series reactive compensation has rarely been used other than on long transmission lines due to the high cost and complexity of implementation. Finally, one can realize a combination of shunt-series devices such as the universal power flow controller that can provide a myriad of control possibilities, but of course at a higher price.

While FACTS devices have been proven technically and have been available for over a decade, market adoption of the technology has been poor. This seems to be largely due to high cost and reliability/availability levels that may not have met utility expectations. High stresses, particularly under fault conditions, and long mean time to repair, are major contributors to the unscheduled downtime experienced by FACTS devices.

The increasing performance and decreasing price of electronics, power electronics and communications technologies have transformed entire industry sectors. It is proposed that a similar approach to the implementation of high power FACTS devices can provide a higher performance and lower cost method for enhancing T&D system reliability and controllability, improving asset utilization and end-user power quality, while minimizing system cost and environmental impact.

The concept of distributed FACTS (D-FACTS) devices has recently been proposed as an alternative approach for realizing the functionality of FACTS devices (series FACTS devices in particular), but at lower cost and higher reliability. This paper proposes an approach for classifying D-FACTS devices, and examines the most important design considerations that would guide and limit the application of such devices.

The concept of a distributed series impedance (DSI) that can realize variable line impedance, which helps control active power flow, is used to illustrate the feasibility of a D-FACTS approach. The concept can be further extended to realize a distributed static series compensator (DSSC), using modules of small rated (~ 10 kVA) single phase inverters and a single turn transformer (STT), along with associated controls, power supply circuits and built-in communications capability. These

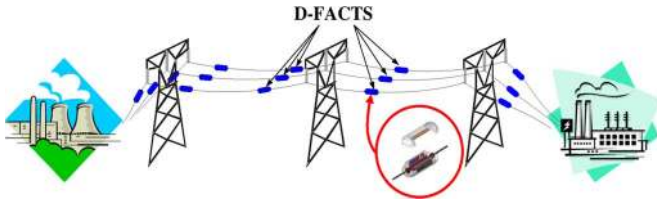


Fig. 1. D-FACTS deployed on power line.

concepts are discussed in detail, along with the benefits and issues associated with such an application.

II. SERIES D-FACTS DEVICES

Fig. 1 shows a conceptual schematic of D-FACTS devices deployed on a power line to alter the power flow by changing the line impedance. Each module is rated at about 10 kVA and is clamped on the line, floating both electrically and mechanically. Each module can be controlled to increase or decrease the impedance of the line, or to leave it unaltered. With a large number of modules operating together, it is possible to have a significant impact on the overall power flow in the line. The low voltampere ratings of the modules are in line with mass manufactured power electronics systems in the industrial drives and uninterruptible power supply markets, and suggests that it would be possible to realize extremely low cost. Finally, the use of a large number of modules results in high system reliability, as system operation is not compromised by the failure of a small number of modules.

Equation (1) shows how power flow varies with the line reactance. Control of real power flow on the line thus requires that the angle δ or the line impedance X_L be changed. A phase shifting transformer can be used to control the angle δ . This is an expensive non-scalable solution and provides limited dynamic control capability. Alternatively, a single series compensator can be used to increase or decrease the effective reactive impedance X_L of the line, thus allowing control of real power flow between the two buses. The impedance change can be effected by series injection of a passive capacitive or inductive element in the line. Alternatively, a static inverter can also be used to realize a controllable active lossless element such as a negative or positive inductor or a synchronous fundamental voltage that is orthogonal to the line current

$$P_{12} = \frac{V_1 V_2 \sin \delta}{X_L} \quad (1)$$

where V_1 and V_2 are the bus voltage magnitudes, δ is the voltage phase difference, and X_L is the line impedance.

The concept of D-FACTS presents the highest potential to increase power flow and consequently the transfer capacity of a meshed transmission, subtransmission, and distribution network. In a meshed T&D network, the power transfer capacity of the system is constricted by the first line that reaches the thermal limit. The inability to effectively control power flow in such a network results in significant underutilization of the overall system. D-FACTS devices offer the ability to improve the transfer capacity and grid utilization by routing

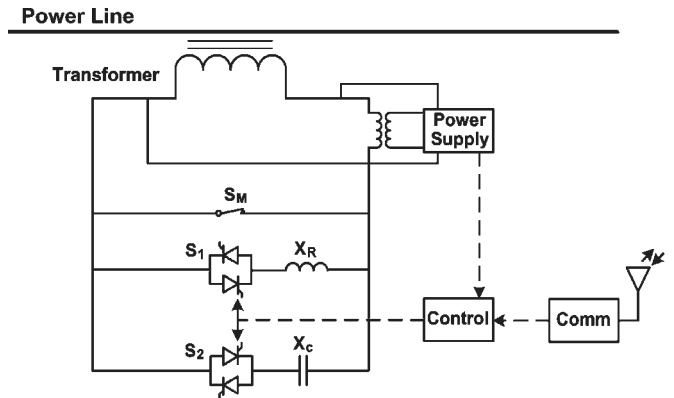


Fig. 2. Generic DSI device.

power flow from overloaded lines to underutilized parts of the network. Capacitive compensation on underutilized lines would make them more receptive to the inflow of the current, while inductive compensation on overloaded lines would make them less attractive to current flow. In both cases, the throughput of the system is increased by diverting additional power flow from the congested parts of the network to the lines with available capacity.

The series injection of impedance or voltage at each module can be accomplished using a STT and a switch. A typical DSI device implementation is shown in Fig. 2. The STT is normally bypassed by the normally closed electromechanical switch S_M , while opening it allows the injection of the desired impedance. Switch S_1 can be closed to inject an overall inductance X_R , while S_2 can be closed to inject capacitance X_C . Control power needs to be derived from the line itself or from the voltage generated across the transformer. Furthermore, the system requires a cost-effective communication infrastructure such as a power line-based communication system for it to be able to function in a coordinated manner.

A higher level of flexibility and dynamic performance can be obtained if a single phase inverter is used to provide injection of a controllable positive or negative inductance, or for the injection of a desired leading or lagging quadrature voltage. The circuit schematic and conceptual implementation of such a system is shown in Fig. 3. This is referred to as the distributed static synchronous compensator. It also utilizes a STT with a normally closed switch S_M that maintains the unit in bypass mode until the inverter is activated. The dc control power supply is excited by the current that flows in the STT secondary winding. As the switch S_M is turned off, the inverter dc bus is charged up and the inverter operation is initiated. The inverter can now inject a quadrature voltage into the ac line to simulate a positive or negative reactance. Furthermore, the ability of the inverter to emulate any impedance or voltage clearly provides higher granularity in terms of system control.

Control of the generic DSI or DSSC devices in Figs. 2 and 3 can accomplish an increase or decrease of line impedance. This clearly requires extraneous information from the rest of the power grid, and indicates the need for a communication system. System operators will provide control input to the DSI system, commanding an increase or decrease in the line

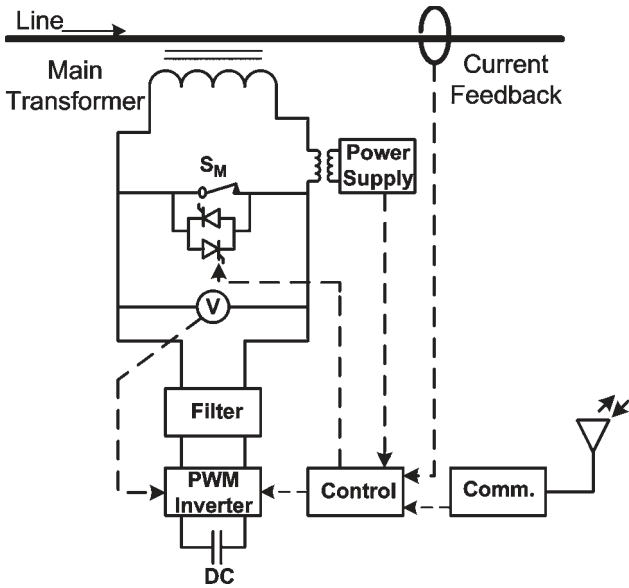


Fig. 3. Generic DSSC device.

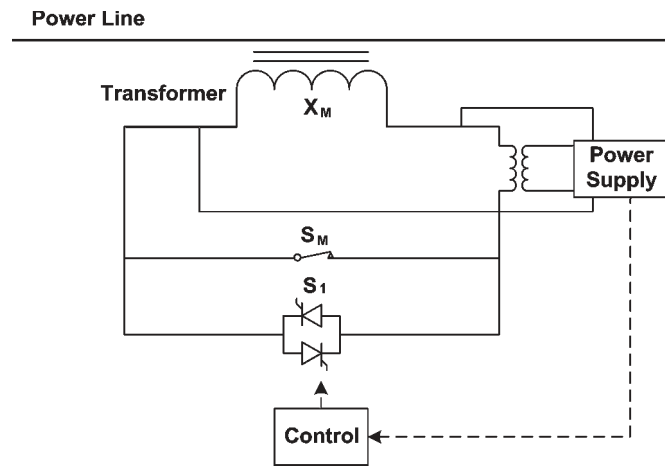


Fig. 4. Circuit schematic of DSR.

impedances to meet system objectives. The communication system clearly adds another layer of complexity and cost to the overall system. If the communication system is eliminated, it will not be clear if the system can be usefully controlled. However, if one considers a more limited functionality, i.e., the ability to only increase the line impedance, it is possible to eliminate communications. One example of such a “limited system” is a distributed series reactor (DSR), as shown in Fig. 4 [10].

As in the case of the DSI, a normally closed electromechanical switch (S_M) is used to bypass the module when it is not energized. With S_M open, the STT magnetizing inductance, tuned to the desired value by setting the air-gap, is inserted into the line. With S_M closed, a minimal level of reactance, corresponding to the STT leakage reactance, is inserted in the line. S_1 is a thyristor switch, which is used to provide a subcycle response, to bypass the module quickly, once a fault is detected. It can be seen that the DSR system has minimal components and complexity, and minimal cost.

TABLE I
LINE PARAMETERS

Operating Line Voltage	Thermal Capacity	Outside radius of conductor	Impedance per mile
138 KV	750 A	0.03 m	0.168+j 0.789

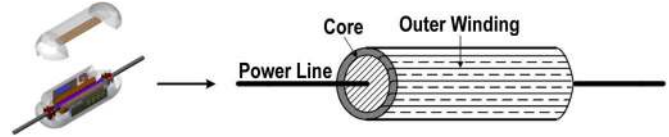


Fig. 5. Single-turn coaxial transformer.

The most important issues concerning the design of such modules are driven by the unique aspects of the application. The issues of mechanical clamping, potential for conductor damage, heat removal, extreme environments, corona discharge, fault currents and lightning strikes are all critical issues that should be resolved. From a module and system control perspective, there are several key issues to address. Operation of the system under normal and fault conditions, coordinated switching of multiple units to achieve a desired control objective, total system weight, and effective heat transfer to the surroundings will determine the efficacy of system operation. Some of these important design considerations are addressed in this paper.

III. TRANSFORMER DESIGN

The STT perhaps represents the most important design issue for series D-FACTS systems. For a typical transmission and distribution line operating at 138 kV level, the line parameters are shown in Table I [5], [6].

The critical parameter for realizing a DSR module is its weight. Based on detailed discussions with utility engineers, a module weight of 50–65 kg is deemed acceptable. A realistic system would be rated at approximately 10 kVA per module, injecting for instance 14 V at 750 A, corresponding to 50 μ H per module. One DSR module per phase per mile could change the line impedance by roughly 2%. A number of such standard modules can be suspended from the power line to realize the required change in the line impedance.

The transformer operation can be categorized under two different operating conditions: bypass mode and the injection mode. In the bypass mode, the output of the transformer is shorted by an electromechanical relay to cancel the power line MMF, and to inject the leakage inductance of the STT into the line. The leakage inductance is very small (approximately 1–2 μ H or 2%–4% of magnetizing inductance) and has practically no effect on the current flow. In the injection mode, the electromechanical relay is opened and the magnetizing inductance X_M is injected into the line.

The transformer core consists of two parts that can be physically clamped around a transmission line, forming a complete magnetic circuit as shown in Fig. 5. The power line itself functions as one of the windings of the transformer. The other winding is wound on the cylindrical core with multiple turns to transform the operating line amperes to a lower value sustainable for the switches under bypass mode.

TABLE II
CORE GEOMETRIES FOR 50- μ H MAGNETIZING INDUCTANCE

Rel. Perm.	MATLAB Inductance (μ H/m)	Inner Radius (cm)	Outer Radius (cm)	Air Gap (cm)	Height (cm)	Weight (Pound)
5000	12.3	2.5	3	0.05	359.7	52.3
	23.9	2.5	3.5	0.05	206.1	65.3
	35.37	2.5	4	0.05	148.6	76.6
	46.7	2.5	4.5	0.05	117.1	86.6
	57.93	2.5	5	0.05	97.8	96.9
	69	2.5	5.5	0.05	84.9	107.7
	80	2.5	6	0.05	75.6	118.9
5000	6.63	2.5	3	0.1	472.1	68.6
	12.65	2.5	3.5	0.1	296.7	94.1
	18.64	2.5	4	0.1	224.2	115.5
	24.59	2.5	4.5	0.1	185.2	137.0
	30.51	2.5	5	0.1	158.7	157.3
	36.4	2.5	5.5	0.1	141.6	179.6
	42.25	2.5	6	0.1	130.5	205.2
5000	12.13	3	3.5	0.05	372.9	64.0
	23.605	3	4	0.05	209.6	77.5
	34.95	3	4.5	0.05	151.6	90.1
	46.16	3	5	0.05	119.0	100.6
	57.26	3	5.5	0.05	99.0	111.1
	68.23	3	6	0.05	85.5	122.0
5000	6.56	3	3.5	0.1	479.4	82.3
	12.55	3	4	0.1	301.2	111.4
	18.5	3	4.5	0.1	226.2	134.5
	24.42	3	5	0.1	185.8	157.1
	30.31	3	5.5	0.1	158.6	178.1
	36.17	3	6	0.1	140.1	200.0

All flux produced by the secondary winding links the primary winding completely. The converse is true if the permeability of the magnetic medium is much higher than that of the insulating material between the primary winding and the magnetic core. The leakage inductance is therefore primarily accounted for from the leakage flux of the primary winding and from the leakage flux of the end turns of the secondary winding.

The weight of the STT core is the most critical design parameter. Since the volume of a cylindrical object varies linearly with the length but not with the square of the radius, a lower weight can be obtained if the length is made much longer than the radius for a given volume [7]. For the same reason, the gap between the cable and the inner radius of the core must be at a minimum to allow enough space for the mechanical clearance and cable deflection under sag conditions. The weight of secondary windings will increase as the length of the core is made longer. However, the increase does not present a significant impact on the overall weight of the module.

The current flowing in the power cable produces flux lines, which are tangential to circular paths around the cable. If the permeability of silicon steel is assumed to be much higher than the air, most of the flux lines can be assumed to be concentrated in the core. The concentration of flux lines in the magnetic core tends to increase the self inductance of the power line, which in turn has the effect of increasing the overall line inductance. The

self inductance of the power line with a magnetic core around it can be calculated from the inverse of the total reluctance faced by the magnetic flux lines. The reluctance of the magnetic path with a thickness " Δr " and at a distance " r " from the power line is given by (2). The total reluctance is given by the parallel combination of the reluctances of incremental thickness " Δr "

$$R = \frac{2\pi r}{\mu(\Delta r * l)} \quad (2)$$

where, μ is the permeability of the magnetic core, and l is the length of the core.

For the particular application of coaxial transformers considered here, the magnetic path of the core will always have a small air gap, as a result of the separable cores needed for clamp-on. The air gap is desired and can be tuned to get the final value of magnetizing inductance. As a first-order design procedure, various core geometries were simulated in MATLAB using (2), with a constant relative permeability of silicon steel at 5000. Table II shows the core geometries and their impact on the weight of the system. The selected core geometry is highlighted in the table and gives 46.7 μ H of magnetizing inductance at 86.6 lb. The basis for selecting this particular geometry was to keep the weight of silicon steel less than 90 lb (41 kg), to achieve the target weight of 120 lb (54.5 kg) for the entire unit.

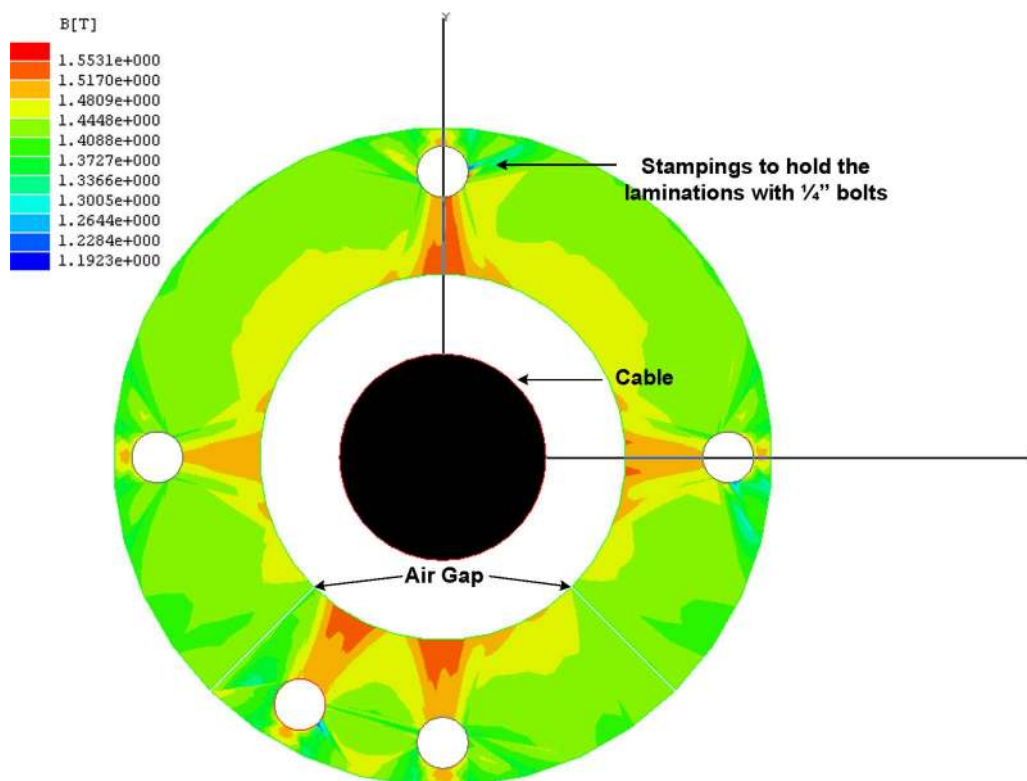


Fig. 6. Magnetizing inductance as a function of line current.

TABLE III
CORE CONFIGURATION

Mechanical Clearance	Inner Radius	Outside Radius	Length	Weight of iron
0.005 m	0.025 m	0.045 m	1.17 m	40 Kg

The selected core geometry was then simulated in MAXWELL finite element package to validate the design. Again, a constant permeability of 5000 was assumed for silicon steel. With this, the magnetizing inductance of the core was obtained as 48.5 μH at 750 A. Finally, the actual nonlinear B–H curve of the commercially available grain-oriented silicon steel was used to account for the saturation effect at high currents. The magnetizing inductance of the transformer was found to be 47.15 μH at a peak current of 750 A. A peak flux density of 1.55 T is observed at the inner circumference (Fig. 6). The physical design of the core is given in Table III.

The design of the secondary winding is primarily governed by the open circuit voltage that switches can withstand, and the sustainable level of current under normal and faulted conditions. The electromechanical relay is the most critical component, as the electrical rating of the relay has a direct bearing on its size and weight. Relays compatible with the size and weight considerations can withstand an OFF-state voltage of 480 V and a continuous current of 30 A. Under an operating current of 750 A, 47.6 μH of primary inductance reflects as 13.5 V on the primary. This suggests a turns ratio of 25 : 1 for the transformer to bring the open circuit voltage to 336 V on the secondary, well within the blocking capability of the relay. The steady state line current of 750 A is reduced to 30 A, which can again be

sustained by the relay. The outer winding also needs to handle the short time fault current of up to 30 000–50 000 A. For the designed length and thickness of the core, a copper wire of 10 AWG is selected. The wire can have nine turns per inch giving sufficient space to have 25 turns on the core. Furthermore, a three-cycle withstand current rating of 2457 A allows for short duration fault currents of 50 000 A on the primary [8]. The weight of the copper in the secondary winding comes out to be 1.39 kg, making the total weight of the transformer to be approximately 41.39 kg. The weight of switches, power electronics, control circuitry, mechanical clamps and the outer casing is estimated to be less than 12 kg, resulting in a total weight of approximately 54 kg.

A. Thermal Model for Losses

Heat generated in the transformer and the module itself must be transferred to the surroundings effectively to maintain safe operation of the windings and the magnetic core. This needs to be done without any fans or moving parts, and the device should be able to withstand climatic extremes and temperatures. There are three different sources of heat generation in the transformer: 1) copper losses in the inner winding, which are present in the bypass as well as injection mode; 2) iron losses in the core, which occur only during the injection mode; and 3) copper losses in the outer winding during the bypass mode. Fig. 7 shows the thermal model of the transformer in the bypass and the normal injection mode. Heat transfer mainly occurs through conduction till the outer surface of the core and through convection from the outer surface of the core

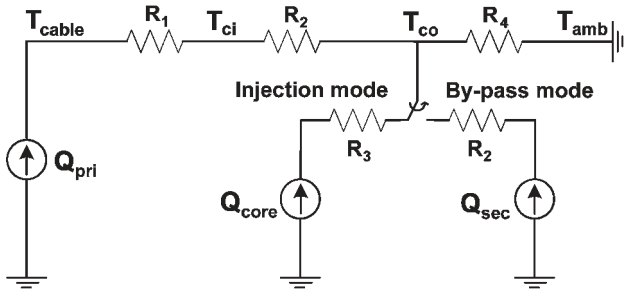


Fig. 7. Thermal model of the transformer.

TABLE IV
POWER LOSS INSIDE THE TRANSFORMER

Core Loss	Cable Loss	Winding Loss
140 W ^a	93.1 W	155.6 W

a. For grain oriented silicon steels, core loss at 1.6 T is around 3.5 W/Kg (Integral Tech., India).

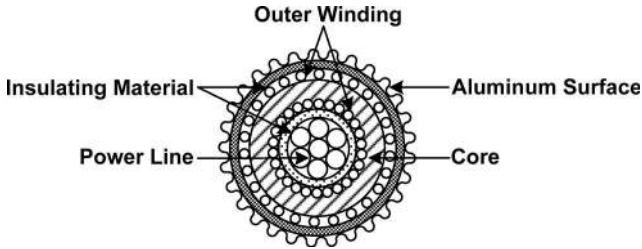


Fig. 8. Front view of the transformer showing aluminum ridges.

to the surroundings. Equation (3) defines the various thermal resistances [9]

$$\begin{aligned}
 R_1 &= \frac{\ln(r_{ci}/r_{cable})}{2\pi\lambda_1 L_c} \\
 R_2 &= \frac{\ln(r_{co}/r_{ci})}{2\pi\lambda_2 L_c} \\
 R_3 &= \frac{(r_{co}^2 - r_{ci}^2)}{4\lambda_2} \\
 R_4 &= \frac{1}{hA}
 \end{aligned} \tag{3}$$

where \$r_{ci}\$ and \$r_{co}\$ are the inner and outer radii of the core, \$r_{cable}\$ is the radius of the cable, \$\lambda_1\$ and \$\lambda_2\$ are thermal conductivities of the insulating material and the core, \$h\$ is the thermal conductance of air, \$L_c\$ is the length of the core, and \$A\$ is the outer surface area of the core.

Table IV gives a summary of the nominal values of power loss in the transformer. With the equations described above, a temperature difference of 4 °C exists between the outer surface of the core and the cable (\$T_{co} - T_{cable}\$). Assuming the cable to be operating at 80 °C, the temperature at the outer surface of the core is 76 °C. Heat transfer through convection depends to a large extent upon the geometry and surface area of the body. Therefore, to increase the heat transfer to the surroundings, the surface of the core is covered with a ridged aluminum surface as shown in Fig. 8. However, one has to ensure that the ridged surface does not cause extensive corona activity, leading to damage of the device.

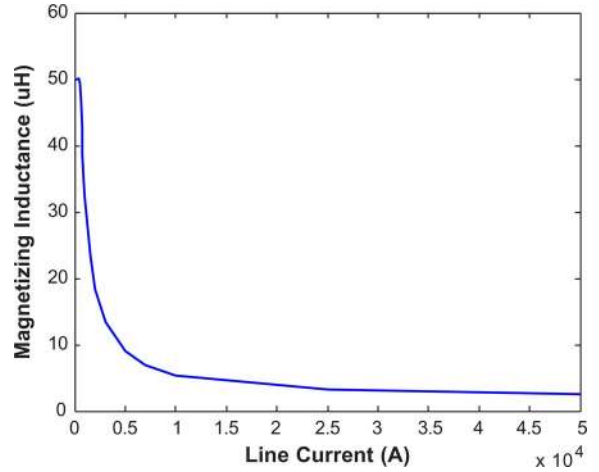


Fig. 9. Magnetizing inductance as a function of line current.

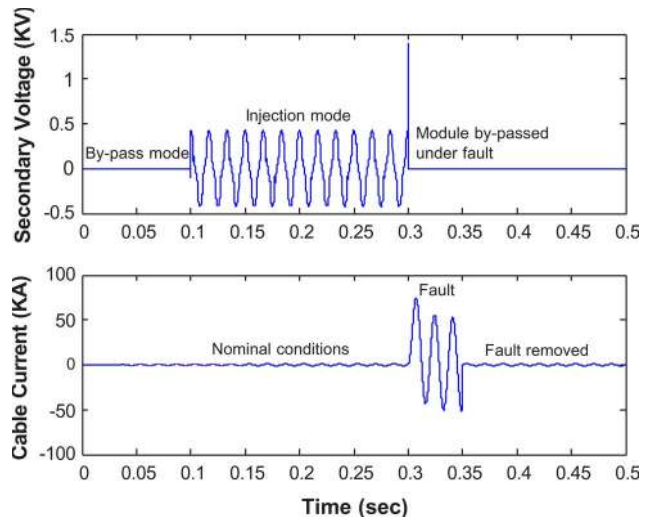


Fig. 10. Operation under bypass, normal injection, and fault conditions.

B. Operation Under Normal and Fault Modes

Fault currents can be as high as 50 000 A, which can cause big voltage spikes on the secondary of the transformer. These voltage transients can be damaging for the switches and control circuitry and is thus desirable that the module switches over to bypass mode once the fault is detected. A thyristor switch is used to quickly bypass the module under fault conditions. Saturation of the transformer also provides a benign layer of protection. Though undesirable under steady state conditions, transformer saturation aids in limiting the voltage induced on the secondary under high currents. Fig. 9 shows the drop in magnetizing inductance as the line current is increased from normal operating conditions to a fault level of 50 000 A.

Fig. 10 shows the simulation results during the bypass, normal injection and fault conditions for a DSI device. The STT was modeled with a magnetizing inductance of 50 \$\mu\text{H}\$ and with a small leakage of 1 \$\mu\text{H}\$. When a fault condition is detected, the system automatically switches over into bypass mode. However, a large voltage transient occurs on the secondary of the STT as the transition is made. For an operating current

of 750 A, followed by a fault current of 50 000 A (75 000 A peak) on the power line, a worst case peak transient voltage of 1.4 kV is generated across the secondary of the STT, which is sustainable for the commercially available power electronic switches. Voltage suppressors will also be provided to limit the transient voltage induced on the secondary and to protect the semiconductor switches.

A secondary protection is also provided in terms of a break-over device, attached between the outer casing of the transformer and the cable to provide an alternate path to current flow under fault conditions or lightning strikes. Detailed design and analysis of device protection will be presented in a future paper.

IV. CONTROL AND OPERATION OF DSR DEVICES

Preselected lines that are likely to see overload conditions at certain times of the day or under defined contingency conditions can be modified with DSR modules to automatically increase the line impedance when thermal overload occurs, transferring the current to relatively uncongested lines of the network. To realize an effective range of control, one can use multiple devices on the line, with each module tuned to “switch-on” at a slightly different precalculated value of the line current. Thus, if a total of 50 DSR modules are used on a single power line, the line impedance could be increased to $50 X_M$, with a resolution of 2%. This allows the power line itself to function like a current limiting conductor [10]. Redundancy introduced by the large number of modules also ensures that a single device failure would have minimal impact on the overall functionality.

A control algorithm for DSR device operation is defined in (4). It requires no communications as the devices operate autonomously, based on the measured line current. A microprocessor-based controller within each module is programmed to turn on the module as the current through the line reaches the triggering value. The control strategy thus allows independent switching of the modules at predefined line currents. Damping is provided by making the desired inductance injection profile to follow an exponential time curve. The value of the exponential at every sampling instant gives the actual value of the inductance to be injected. The trajectory of the injected inductance over an interval of Δt sec is described by (5), and the numbers of modules corresponding to the value of the exponential are turned on at every sampling instant. Detailed discussion on the control strategy and line interactions can be found in an earlier paper [10]. The profile of injected impedance will be as shown in Fig. 11

$$L_{inj} = L_f \frac{(I_{line} - I_0)}{(I_{thermal} - I_0)} \quad (4)$$

where L_{inj} is the injected line inductance, L_f is the final value of inductance with all the DSR modules on the line active, I_0 is the triggering value of the current for a module, and $I_{thermal}$ is the thermal limit beyond which there is no injection

$$L_{exp} = (L_{inj} - L_{prev}) \left(1 - \exp^{-(t-t_0)}\right) + L_{prev} \quad (5)$$

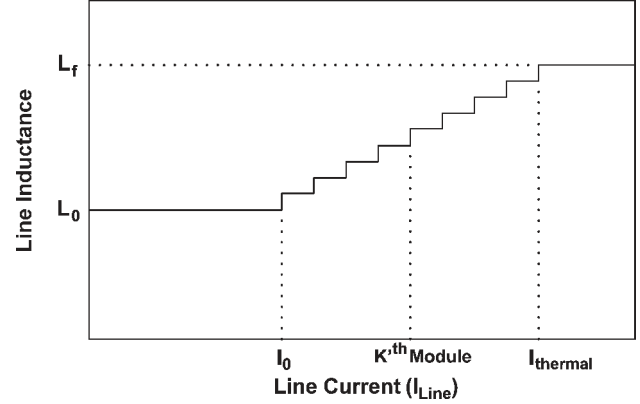


Fig. 11. Profile of injected impedance.

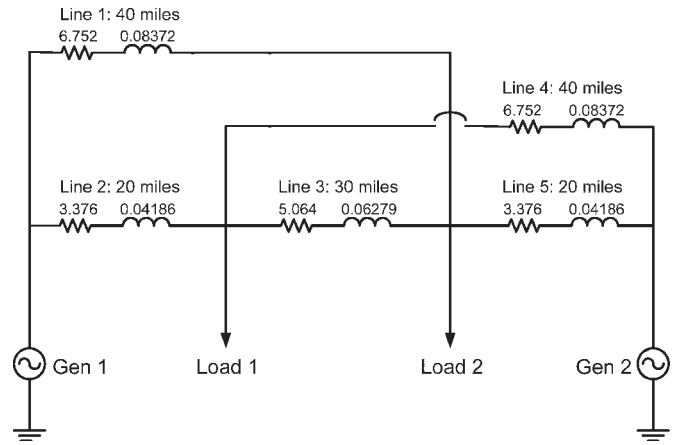


Fig. 12. Detailed schematic of the four-bus system.

valid over $t_0 \leq t \leq t_0 + \Delta t$, where L_{exp} corresponds to actual injection at the end of every sampling instant, and L_{prev} corresponds to the injection at the previous instant.

V. SIMULATION RESULTS

As an example illustrating DSI operation in a system, the ability of DSR devices to alleviate line loading and congestion was simulated with the simple four-bus system shown in Fig. 12. Each of the lines has a thermal rating of 750 A and an impedance of $0.168 + j 0.789$.

Line 2 and Line 5 are identified as the most critical line of the network as the maximum transfer capacity of the network is determined by these lines. Fig. 13 shows Line 2 operating at the thermal limit, with a rapid reduction in average current as the DSR devices are switched on. The redistribution of the current through the network has a direct impact on the available transfer capacity (ATC). The original system ATC is limited by Line 2 or Line 5. However, with the deployment of DSR modules, an increase in the load throughput by as much as 75% can be realized when the load is concentrated at Load 1 (Fig. 14). This shows the ability of the DSR devices to automatically control the level of current in the grid, automatically operating to keep power lines out of thermal overload.

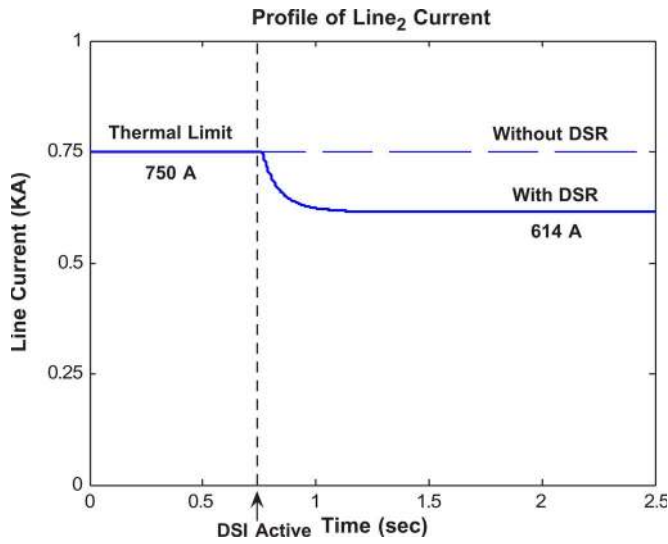


Fig. 13. Profile of Line 2 current under overload.

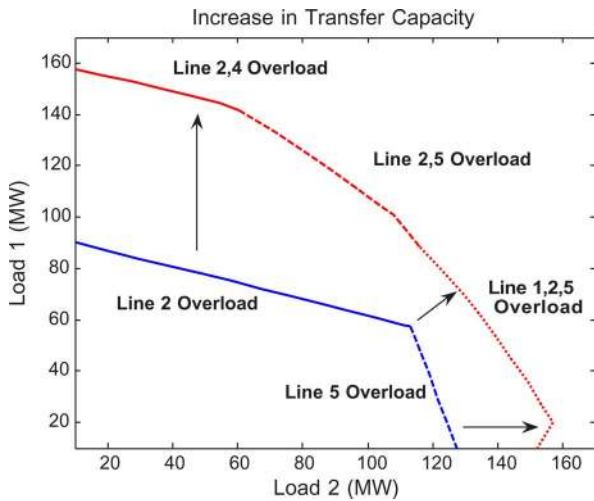


Fig. 14. Increase in ATC of the system.

The concept has been applied to a more complex network such as the IEEE 39 Bus System, and the studies show that the modules operate with minimal interaction with each other. The results will be discussed in a future paper.

VI. EXPERIMENTAL RESULTS

To demonstrate the concept of D-FACTS devices, a DSSC module was built and tested in the laboratory under a project jointly funded by TVA and Soft Switching Technologies [11]. A circuit schematic of the system is shown in Fig. 15, and the lab prototype is shown in Fig. 16. The DSSC system was capable of injecting leading or lagging impedances or quadrature voltages, and could balance the dc bus voltage on the single phase inverter using an “in-phase” component of the voltage. Successful operation was demonstrated in a laboratory environment. Details of the results have been presented in a previous paper, and are summarized here [11].

The unit was designed for line currents of up to 1500 A and fault currents of over 12 000 A. The insulated gate bipolar

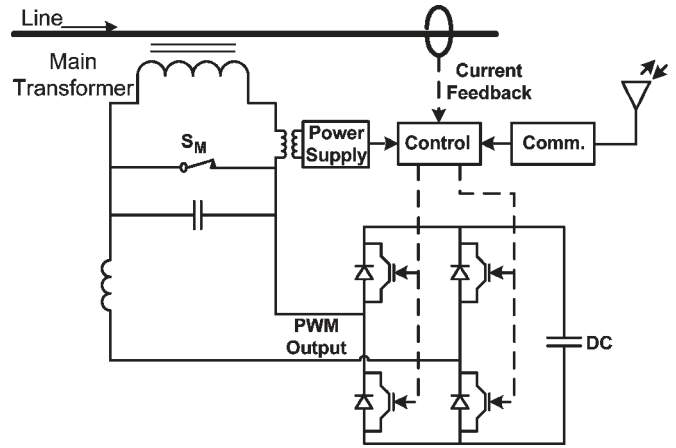


Fig. 15. Circuit schematic of DSSC.

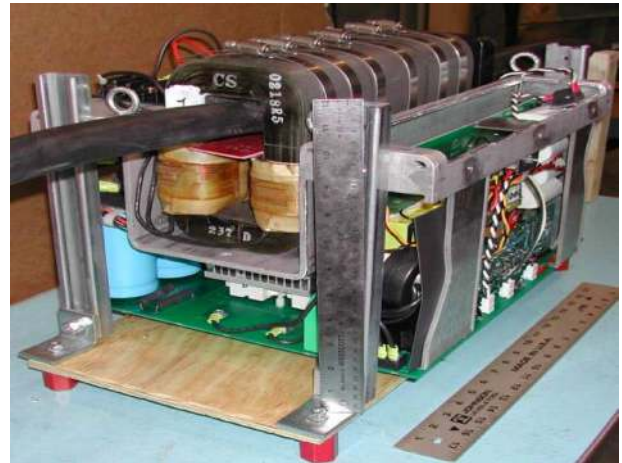


Fig. 16. Laboratory prototype of DSSC.

transistor (IGBT) inverter was rated at 6.7 kVA and was used to provide the fault current ride-through capability. Based on an STT turns ratio of 90:1, the nominal current in the IGBT inverter at 1500 A was less than 20 A. The inverter devices were controlled using sine-triangle pulsewidth modulation at 12 kHz using a peripheral interface controller (PIC) microcontroller. DC bus control was realized using a signal in-phase with the line current, while a command reference signal provided the desired quadrature voltage injection. The power supply was designed to operate over a range of 300–1500 A in steady state, with ride-through for current surges up to 12 000 A. The module demonstrated injection of positive and negative inductance, quadrature voltage of ± 4.6 V, and the ability to steer power flow through a desired path in a parallel connection.

Figs. 17 and 18 shows DSSC operation under zero, leading and lagging voltage injection conditions. With zero injection, the voltage impressed across the STT is seen to be in-phase with the current, corresponding to losses in the circuit. The DSSC module was tested under normal and fault currents of up to 12 000 A, and behaved as anticipated. Finally, the DSSC module was used to demonstrate the ability to steer current between two parallel lines as commanded (Fig. 19).

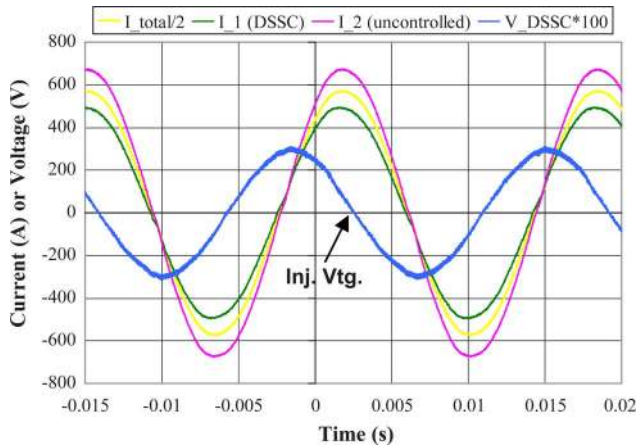


Fig. 17. Operation under leading voltage injection.

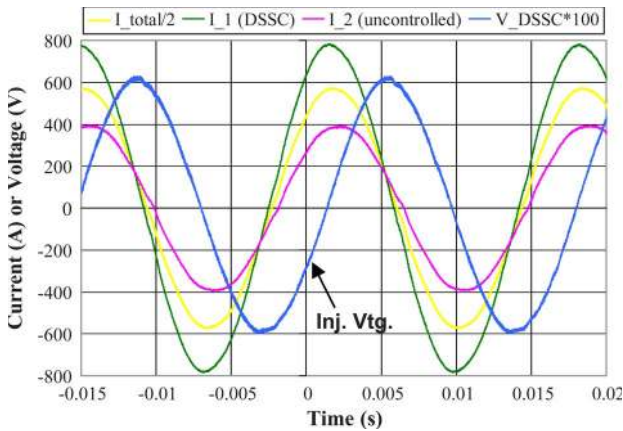


Fig. 18. Operation under lagging voltage injection.

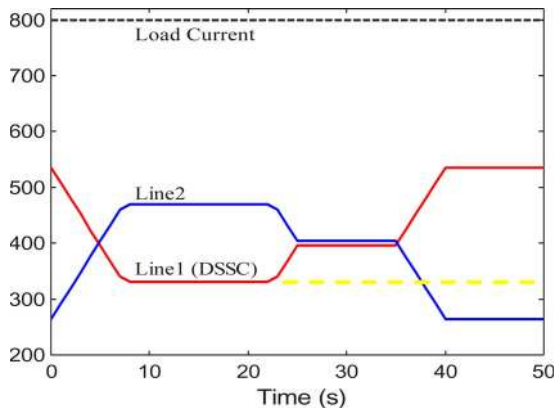


Fig. 19. Line current steering with DSSC.

VII. CONCLUSION

This paper has presented a new approach to controlling power flows in transmission and distribution grids. D-FACTS devices using commercially available low power devices, offer the potential to dramatically reduce the cost of power flow control. Series var compensation using D-FACTS would help utilities alleviate grid congestion, defer construction of new transmission lines, and improve system capacity. D-FACTS

devices require no change in utility infrastructure and operate autonomously, with or without communications. The high reliability, low cost and long life of these devices make them all the more attractive.

Widespread adoption of this technology requires in-depth analysis of some of the practical limitations. Some of the issues such as operation under normal and fault conditions, coordinated switching, heat transfer and total system weight have been addressed in this paper. Simulations and experimental results demonstrate the potential impact of these devices in terms of better grid utilization and improvement in system reliability.

REFERENCES

- [1] S. Abraham. (2002, May). *National Transmission Grid Study*. Washington, DC: U.S. Dept. Energy, [Online]. Available: <http://www.eh.doc.gov/ntgs/>
- [2] N. Hingorani, "Flexible AC transmission," *IEEE Spectr.*, vol. 30, no. 4, pp. 40–45, Apr. 1993.
- [3] L. Gyugyi, C. D. Schauder, and K. K. Sen, "Static synchronous series compensator: A solid-state approach to the series compensation of transmission lines," *IEEE Trans. Power Del.*, vol. 12, no. 1, pp. 406–417, Jan. 1997.
- [4] M. Noroozian and G. Andersson, "Power flow control by use of controllable series components," *IEEE Trans. Power Del.*, vol. 8, no. 3, pp. 1420–1429, Jul. 1993.
- [5] A. Bergen, *Power System Analysis*. Englewood Cliffs, NJ: Prentice-Hall, 1986.
- [6] Westinghouse Electric Corporation, *Electrical Transmission and Distribution Reference Book*, 1950.
- [7] M. Rauls, "Analysis and design of high frequency co-axial winding power transformers," M.S. thesis, Univ. Wisconsin, Madison, 1992.
- [8] R. C. Mullin and R. L. Smith, *Electrical Wiring Commercial*. Albany, NY: Thomson Delmar Learning, 2004.
- [9] F. Kreith, *Principles of Heat Transfer*. Scranton, PA: Int. Textbook, 1958.
- [10] H. Johal and D. Divan, "Current limiting conductors: A distributed approach for increasing T&D system capacity and enhancing reliability," in *Proc. IEEE PES Transmiss. Distrib. Conf. Expo.*, May 2006, pp. 1127–1133.
- [11] D. Divan, W. Brumsickle, R. Schneider, B. Kranz, R. Gascoigne, D. Bradshaw, M. Ingram, and I. Grant, "A distributed static series compensator system for realizing active power flow control on existing power lines," *IEEE Trans. Power Del.*, vol. 22, no. 1, pp. 642–649, Jan. 2007.



Harjeet Johal (S'06) received the B.S. degree in electrical power engineering from the Indian Institute of Technology, New Delhi, India, in 2003. He is currently working toward the Ph.D. degree at Georgia Institute of Technology (Georgia Tech), Atlanta, under the supervision of Dr. D. Divan.

He has been a Teaching Assistant for five semesters and a Research Assistant for four semesters at Georgia Tech. His research focuses on increasing T&D system capacity and enhancing reliability.

He is working on modeling distributed series impedances, which can be used to alter the line flow in a meshed power network to maximize the transfer capacity and network utilization. His research aims at developing passive clip-on modules that automatically increase the impedance of the line once a current threshold is reached, diverting current to other unloaded parts of the network.

Mr. Johal is a Corecipient of the 2005 IEEE Power Electronics Specialists Conference Best Paper Award. He was also awarded with the best undergraduate project award in 2003.



Deepak Divan (S'78–M'78–SM'91–F'98) received the Bachelors of Technology degree from the Indian Institute of Technology, Kanpur, India, in 1975, and the Master's and Ph.D. degrees from the University of Calgary, Calgary, AB, Canada, in 1979 and 1983, respectively.

From 1985 to 1995, he was a Professor with the Department of Electrical and Computer Engineering at the University of Wisconsin, Madison. He was also Associate Director of the Wisconsin Electric Machines and Power Electronics Consortium, the first university–industry consortium on campus that he helped to grow to include over 60 industrial sponsors. In 1995, he started Soft Switching Technologies and as President, CEO, and Chairman of the Board, he was responsible for raising venture capital funding from leading investors including GE Capital and JP Morgan Partners, for developing a line of power line disturbance monitoring and mitigation products to help factories avoid costly unscheduled downtime, and for positioning the company as a leader in this emerging market. From 2003 to 2004, he served as Chairman and Chief Technology Officer for the company, successfully transitioning company operations to an experienced management team. He joined Georgia Institute of Technology (Georgia Tech), Atlanta, in 2004 to create a strong program in the application of power electronics and related technologies to power systems and demanding defense and industrial applications. He is the holder of 32 patents, has published approximately 200 technical papers, including over 12 prize papers, and has given many invited presentations at technical- and business-oriented meetings. He is currently the Director of Intelligent Power Infrastructure Consortium, a university–industry–utility consortium that has been formed to provide a focal point for the academic teaching and research program in advanced power technologies at Georgia Tech.